Investigating the impact of Metformin on proliferation in mitochondria-depleted MDA-MB-231 BC cells.

Bibinur Kenzhetay

PI: Mohammad Aljofan

Co-PI: Agata N Burska

Nazarbayev University

Astana, Kazakhstan

TABLE OF CONTENTS

INTRODUCTION

1.1 Epidemiology of BC in Kazakhstan

BC (BC) ranks as the 5th leading cause of cancer-related deaths worldwide. According to 2020 data from GLOBOCAN, (BC) is the most frequently diagnosed cancer in women, accounting for approximately 11.7% of total cases, with 2.3 million new cases annually - surpassing previously leading lung cancer. BC represents 1 in 4 cancer cases and 1 in 6 cancer deaths among women, ranking first in incidence in the vast majority of countries (Sung et al., 2021).

Similarly, to the majority of countries, in Kazakhstan BC ranks first in the new cases for malignant neoplasms in women, with incidences of 4.6 thousand, and mortality of 1.3 thousand registered annually. According to Dunenova et al. (2023) the number of BC cases registered annually has increased by 46.9% from 2014 to 2019 possibly due to the introduction of international standards for BC screening in 2012 (e.g. double reading of mammograms, interpretation via BIRADS system, comparison of detected cases of BC with Electronic Registry of Cancer Patients), and expansion of age groups eligible for screening from 50-60 years old in 2008, to 40-70 years old in 2017.

1.2 Types of BC

The ongoing advancement of medicine has identified six major hallmarks of carcinogenesis: evasion of apoptosis, self-sufficiency in growth signals, insensitivity to anti-growth signals, sustained angiogenesis, tissue invasion and metastasis, and limitless replicative potential (Hanahan, 2022). Cancer can develop in any cell, tissue, or organ, and cancer-related deaths continue to rise annually. BCs are subdivided into four major categories based on mRNA gene expression levels: Luminal A, Luminal B, HER2-enriched, and basal-like. Luminal A subtype is the most common tumor found in breast tissue, comprising around 70% of all cases. They are characterized by the presence of both or one of the Estrogen- or Progesterone-receptors,

and have marginally better prognosis due to the low amount of cell proliferation genes, clinically are considered slow-growing, and low-grade (Park et al., 2011). On the other hand, Luminal B subtype has high expression of those genes (i.e. MKI67), ER-positive, and can be with PR-negative and/or HER2-positive with is clinically predictive of a worse prognosis. HER2-enriched subtype cancers grow faster than both Luminal subtypes, and were previously indicative of the worst prognosis, but after the introduction of HER2-targeted therapies such as trastuzumab the treatment response was improved. Basal like or triple-negative BC (TNBC) with the worst prognosis is a heterogenous group of ER-/PR- and HER2-negative BCs represent approximately 20% of all BC cases. TNBCs are generally very aggressive and have a high recurrence rate, with a possibility of developing chemoresistance in the next rounds of chemotherapy (Park et al., 2011).

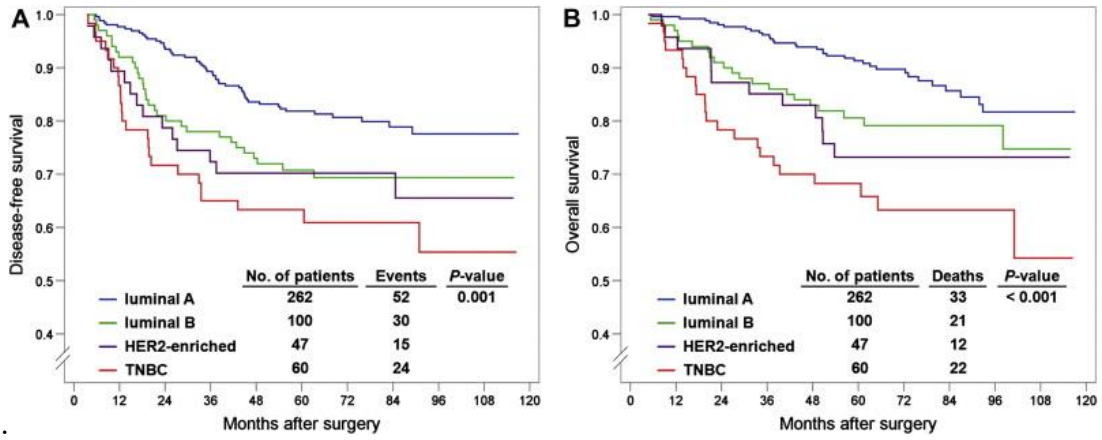

Figure 1. Park et al., 2011Disease-free (A) and overall (B) survival according to molecular subtypes. HER2: human epidermal growth factor receptor type 2; TNBC: triple-negative breast cancer;

1.3 Experimental cellular models used in BC research

BC research is largely based on the knowledge derived from breast carcinoma *in vivo* and *in vitro* cell line models. Several cell line models such as MDA-MB-231, MCF7, T47D are widely used in the laboratory setting, accounting for over 60% of associated preclinical research (Dai et al., 2017). BT20 was the first triple-negative BC cell line that was isolated in 1950s from a

pleural effusion. Later in 1970s many of the currently used cell lines such as abovementioned MDA-MB-231, MCF7, and others (AU565, BT-474, MDA-MB-453, etc.) were established.

Table 1. Common breast cancer cellular models utilized in research

Cell line	**Type (ER/PR/HER2)/subtype**	**Relevance**
MDA-MB-231	(-/-/-)/TNBC	No expression of ER, progesterone receptor, or HER2, highly aggressive Used to study late-stage invasion, metastasis, and chemotherapy resistance (Welsh, 2013).
T-47D	(+/+/-)/Luminal A	Used to study hormone receptor-positive breast cancer and mechanisms of resistance to endocrine therapies. (Yu et al., 2017)
MDA-MB-468	(-/-/-) TNBC	Used in studies focused on TNBC's aggressive behavior, metastasis, and resistance, especially to chemotherapy and immunotherapy (Welsh, 2013).
MCF-7	(+/+/-)/Luminal A	Common cell line for studying ER+ BC. Used to study hormonal therapy responses and mechanisms of resistance to tamoxifen (Hera Biolabs, 2023).
MCF10A	Non-tumorigenic epithelial cell line	Most commonly used cell line for studying normal cellular function *in vitro*, was derived from a human mammary epithelial tissue (Qu et al., 2015).

ER – estrogen receptor, *PR* – progesterone receptor, *HER2* – human epidermal growth factor receptor, *TNBC* – triple-negative breast cancer.

1.4 Mitochondria role in cancer

Mitochondria is the *powerhouse* of the cell. It is primarily responsible for producing adenosine triphosphate (ATP) through oxidative phosphorylation (OXPHOS). In addition to energy production, mitochondrion is involved in various cellular processes such as cell cycle regulation, cell signaling, and apoptosis. Structurally, mitochondrion is comprised of a double-membrane system and a separate genome, distinct from nuclear DNA. This mitochondrial DNA

(mtDNA) is inherited from the maternal mtDNA and encodes for 13 essential OXPHOS genes essential for metabolism, and biogenesis. Oxidative phosphorylation takes place in the inner mitochondrial membrane. This process involves a series of electron transfer reactions that result in the phosphorylation of adenosine diphosphate (ADP) to ATP. In addition to energy production, mitochondria play a critical role in maintaining cellular homeostasis by managing the balance between energy demand and supply, modulation of redox, generation of ROS (reactive oxygen species) which allows mitochondria to adapt to cellular biogenesis and reproduction in rapidly-dividing cells (Wallace, 2012).

1.5 Mitochondria role cellular proliferation

The development of mitochondrial DNA-depleted cells (Rho0) originated from investigations into eukaryotic cellular dependence on oxidative phosphorylation. Early studies in the 1970s demonstrated that prolonged exposure to mitochondrial inhibitors like ethidium bromide could selectively eliminate mtDNA without causing immediate cell death. This critical finding enabled the later creation of stable Rho0 cell lines in the late 1980s by King and Attardi at Caltech, who established a method using low concentrations of ethidium bromide to generate cells completely lacking mtDNA. Their seminal work showed that while mtDNA-encoded proteins are essential for oxidative phosphorylation, cells could surprisingly survive without mitochondrial respiration when provided with uridine and pyruvate supplements in culture media.

The metabolic adaptations of Rho0 cells reveal fundamental insights into cellular energy metabolism. Due to their defective electron transport chain, these cells exhibit two key dependencies. First, they become auxotrophic for pyrimidines because the mitochondrial enzyme dihydroorotate dehydrogenase, required for de novo pyrimidine synthesis, cannot function without an active electron transport system. This necessitates uridine supplementation. Second, Rho0 cells require pyruvate to maintain cytosolic redox balance since they cannot oxidize

NADH through mitochondrial shuttles. Instead, they rely on lactate dehydrogenase to regenerate NAD+ by converting pyruvate to lactate. These adaptations mirror the metabolic rewiring observed in many cancer cells, making Rho0 models particularly valuable for studying tumor bioenergetics.

Methodological advances have progressively refined Rho0 cell generation. While early approaches relied on ethidium bromide, later techniques employed nucleoside analogs like ddC to minimize off-target effects (Wallace, 1999). Recent innovations include targeted mitophagy induction and CRISPR-based approaches, offering more precise mitochondrial depletion (Correia-Melo et al., 2017; Khozhukhar et al., 2023). These improvements have enhanced the specificity and reduced potential artifacts in Rho0 studies.

In cancer research, Rho0 cells have provided crucial insights into therapeutic resistance mechanisms. They model how tumors with mitochondrial dysfunction develop resistance to oxidative stress-inducing treatments. Furthermore, Rho0 cells have helped identify compensatory metabolic pathways that could represent novel therapeutic targets. Current applications extend beyond cancer to mitochondrial diseases, aging research, and regenerative medicine.

Emerging technologies continue to expand Rho0 cell applications. The integration of single-cell omics and mitochondrial transplantation techniques is providing unprecedented resolution in studying mitochondrial-nuclear crosstalk (Kukat et al., 2008). These advancements are addressing previous limitations and bridging the gap between cell culture models and physiological systems. Looking forward, combining Rho0 models with organoid systems and advanced imaging promises to yield new breakthroughs in understanding mitochondrial function and dysfunction across biological contexts.

1.6 Antitumoral effects of Metformin

Biguanides are a class of synthetic antihyperglycemic agents, which contain metformin, phenformin, and buformin. These compounds were derived from galegine, the active component of the traditional medicinal plant Galega officinalis L. (Fabaceae), and were utilized in herbal remedies for centuries (Bailey, 2017).

Among the biguanides, metformin is widely prescribed for diabetes as an antihyperglycemic agent. Metformin has a higher safety and efficacy profile than the other medications from the same class. Thus, the use of buformin and phenformin in the 1970s was removed from the counters due to their association with high risk of lactic acidosis and other adverse effects (Bailey, 2017).

Metformin inhibits the mitochondrial respiratory chain on Complex I. This action activates the AMPK pathway while inhibiting the mTOR and the phosphatidylinositol 3-kinase/AKT pathways (PI3K/AKT). Recent research has suggested that metformin may possess antitumoral capabilities (Moldasheva et al., 2024)

Table 2. Metformin Use and Breast Cancer Outcomes.

Study design	Results	References
Cohort Study 68,019 women of the Women's Health Initiative clinical trial population	Diabetic postmenopausal women receiving metformin had lower incidence of invasive BC, whereas women with diabetes receiving other antidiabetic drugs presented a slightly higher incidence.	(Chlebowski et al., 2012).

Case-control. Ontario database of 2361 patients with **BC** diagnosis and metformin treatment	9% reduction in BC-specific mortality per additional year of cumulative metformin use	(Lega et al., 2013)
Case-control. Asian Medical Center's breast database of 7353 patients with resected **BC** and metformin treatment	Patients had significantly better overall and cancer-specific survival	(Kim et al., 2015)

This effect could be directly through activating AMPK, as it activates the same pathways responsible for its antihyperglycemic action, thus resulting in antiproliferative effects on cancer cells or metformin may influence cancer progression indirectly through AMPK-independent mechanisms, such as lowering circulating glucose and insulin levels. This is achieved by enhancing glucose uptake in muscle tissues and inhibiting gluconeogenesis in the liver, thereby creating a less favorable environment for tumor growth due to a lack of nutrients (Choi & Park, 2013).

HYPOTHESIS AND AIMS:

Hypothesis: Metformin exerts distinctive effects on proliferation in mitochondria-depleted MDA-MB-231 breast cancer cell line

Aims:

1. To optimize generation of mitochondria depleted MDA-MB 231 and
2. Investigate the susceptibility of MDA MB 231 Rho0 cells to Metformin.

MATERIALS AND METHODS

2.1 Cell culture

The MDA-MB-231 cell line was used in this study. This cell line was originally derived from a 51-year-old white American woman with metastatic BC. The MDA-MB-231 cell line, including a variant with overexpressed Parkin, was kindly provided by Dr. Agata N. Burska. For Parkin overexpression, HEK 293T (ATCC CRL-11268) were co-transfected with pMXs-IP HA-Parkin retroviral construct (Addgene #38248; encoding HA-tagged human Parkin) and the retroviral packaging plasmids pCL-Ampho (NOVUS Biologicals NBP2-29541) using Lipofectamine 3000 (Thermo Fischer Scientific), following the manufacturers protocol. Target MDA-MB-231 cells were incubated with viral supernatant in the presence of 8ug/mL polybrene (Sigma-Aldrich) for 24 hours. Fresh medium was replaced, and cells were allowed to recover for 48 hours. Transduced cells were selected with 1ug/mL puromycin (Invitrogen) for 2 days, collected and validated by Western bot using an anti-HA antibody, stable expression verified. MDA MB 231 cells were cultured in Dulbecco's Modified Eagle Medium/Nutrient Mixture F-12 (DMEM/F-12, Gibco, USA) supplemented with 10% fetal bovine serum (FBS, Gibco, USA), 1 and 1% penicillin-streptomycin (Gibco, USA) and media for MDA MB 23 Rho0 cells was additionally supplemented with 50ug/mL uridine, and 100ug/mL Sodium Pyruvate. Cells were grown in the incubator at 37°C with 5% CO2 supply. Cells were passaged every 3-4 days, media was changed accordingly, and the experiments were performed with cells from passages 4 to 16.

2.2 Drug treatment

The stock concentration of 1M metformin was prepared containing 12.5% DMSO. Cells were treated with increasing doses of metformin, depending on the experiments the concentration ranged from 0mM-80mM.

2.3 Enforced mitophagy for mitochondria depletion

For mitochondrial depletion via enforced mitophagy MDA-MB-231 Parkin-overexpressing cells were seeded on a 10cm plate at 5*10^5 cells/plate, left in the incubator 37C for 24h to adhere, and later 10uM CCCP was added to the culture every 12h for the total of 48h to induce mitophagy (Correia-Melo et al., 2016). Post-mitophagy the MDA-MB-231 Rho0 cells were cultured in DMEM F-12 supplemented with uridine 50ug/mL, and sodium pyruvate 100ug/mL. The depletion was validated by the assessment of mtDNA copy number.

2.4 Mitochondrial DNA copy number (mtDNA CN) quantification by qPCR

Genomic DNA was isolated from cell pellets, collected after mitochondrial depletion by trypsinization, using PureLink™ Genomic DNA Mini Kit according to manufacturer's protocol. DNA concentration and purity were assessed via spectrophotometry (NanoDrop), with acceptable A260/A280 ratios (1.8–2.0). Samples were diluted to a working concentration of 25ng/µL in nuclease-free water.

Mitochondrial DNA copy number (mtDNA CN) was quantified by SYBR™ Green Universal Master Mix. The mitochondrial gene *ND1* was amplified as the mtDNA target, and the nuclear gene *HMBS* (hydroxymethylbilane synthase) as the nuclear target.

Primer Sequences:

Gene	Direction	Sequence (5′→3′)
ND1	Forward	GGCTATATACAACTACGCAAAGGC
	Reverse	GGTAGATGTGGCGGGTTTTAGG
HMBS	Forward	ACGGCTCAGATAGCATACAAGAG
	Reverse	GTTACGAGCAGTGATGCCTACC

qPCR Reaction mix composition (20 µL final volume):

	Component	Volume/concentration
1	SYBR Green Master Mix (2X)	10 µL
2	Primer (final concentration)	400 nM
3	Template DNA (25ng)	2 µL
4	Nuclease-free water	to 20 µL

Thermocycling Protocol (QuantStudio™ 6 System):

1. Initial denaturation: 95°C for 10 min
2. Amplification (40 cycles):
    - 95°C for 15 sec (denaturation)
    - 60°C for 1 min (annealing/extension)
3. Melt curve analysis: 60°C to 95°C (0.3°C/sec increment)

mtDNA Copy Number Calculation

The relative mtDNA copy number per cell was calculated using the ΔΔCq method (Livak & Schmittgen, 2001):

mtDNA CN=2×2−ΔΔCqmtDNA CN=2×2−ΔΔCq

Where:

- **ΔCq** = Cq(*ND1*) − Cq(*HMBS*)
- The factor 2 accounts for the diploid nature of nuclear DNA (*HMBS*).

Quality Control

- All samples were run in triplicate, with Cq standard deviations (SD) > 0.5 excluded.

- Melt curve analysis confirmed single amplification products.

2.5 Microscopic Observation of Cell Morphology

MDA 231 parental and MDA MB 231 Rho0 cells were cultured in 6-well plates for 24h to adhere. The cells were further incubated with different concentrations of metformin for 24h, and cell morphological changes were observed and photographed by a phase contrast microscope Primovert (Zeiss) using a 10X, 20X, and 40X objectives.

2.6 Cell Viability Assay (MTS Assay)

Cell viability was assessed using the MTS Assay according to the manufacturer's instructions. Briefly, 10,000 cells per well (both parental and Rho0 MDA-MB-231 cells) were seeded in a 96-well plate and allowed to adhere for 24 hours. Cells were then treated with varying concentrations of metformin (0, 5, 10, 20, 30, and 40 mM) for 24 and 48 hours. Following treatment, 10 µL of MTS reagent was added to each well, and the plates were incubated at 37°C for 2–4 hours. Absorbance was measured at 490 nm using a Biorad Mark™ Microplate Absorbance Reader to determine cell viability. The half-maximal inhibitory concentration (IC50) of metformin was calculated using dose-response curves generated from the viability data.

2.7 xCELLigence Real-time Cell analysis

MDA 231 parental and MDA MB 231 Rho0 cells were cultured in 10cm plates for 24 hours, later the cells were collected by trypsinization and counted via Invitrogen Countess 3 Automated Cell Counter. The E16 xCELLigence plates were preconditioned by addition of DMEM F-12 for MDA-MB-231 parental, and media supplemented with uridine and pyruvate for Rho0 cells (100 µL) to every well. Plates were inserted back into the xCELLigence station (Agilent), and the

base-line impedance was measured to ensure that all wells and connections were working within acceptable limits. The cells were seeded 10,000 cells/well into xCELLigence E-plate (E16) for 24 hours to adhere, after which metformin was added at 0mM, 10mM, 20mM, 30mM concentrations and left for 72h to measure Cell Index (CI)/Normalized Cell Index (NCI) – the cell index is the measure of adhesion of cells per individual well. The data was recorded via xCELLigence Software: RTCA Software Pro 2.8.1
for total of 96 hours, including adhesion time.

2.8 Fluorescent Microscopy Observation of Cell Morphology

MDA-MB-231 cells parental, and Rho0 were seeded at a density of 300,000 cells per 35mm confocal dishes and allowed to adhere for 24 h. Following adherence, one set of each condition was treated with 22.23 mM metformin for 24h. Prior to imaging, cells were stained with 1:1500 Hoechst (nuclear staining) and 200 nM MitoTracker Deep Red (MTDR) (mitochondrial staining). Following the manufacturer's washing protocol, imaging was performed using an inverted Zeiss fluorescence microscope equipped with confocal capabilities, and appropriate filter sets were used to capture Hoechst (ex/em ~350/461 nm) and MTDR (ex/em ~644/665 nm) signal.

2.9 Quantification of Cellular ROS by DCFDA assay

Intracellular ROS levels were measured using the fluorescent probe 2',7'-dichlorofluorescein diacetate (DCFH-DA). MDA-MB-231 parental cells and Rho0 cells were cultured in DMEM F-12. For experiments, cells were seeded at a density of 50,000 cells per well in 12-well plates and allowed to adhere overnight. Cells were then treated with metformin at concentrations of 0 mM, 5 mM, 10 mM, 20 mM, 40 mM, and 80 mM in duplicate and incubated for 24 hours.

Following treatment, cells were incubated with 1 uM DCFH-DA, while nuclei were counterstained with Hoechst 1:2000 dilution (Invitrogen, 33342) in FBS-, antibiotic-, and phenol-free media for 20 minutes at 37°C to assess ROS production. After two PBS washes to remove excess dye, cells were immediately imaged using a Zoe Fluorescence Cell Imager. DCF fluorescence (indicative of ROS levels) was detected using the green channel (excitation/emission: 485/535 nm), while nuclear staining was visualized using the blue channel (excitation/emission: 350/461 nm).

Fluorescence intensity was quantified using ImageJ software (National Institutes of Health) by measuring mean pixel intensity of the DCF signal in individual cells and normalizing to cell number as determined by Hoechst staining. Results are expressed as mean fluorescence intensity relative to untreated controls.

RESULTS

3.1 Mitochondrial DNA depletion and morphological changes in MDA-MB-231 Rho0 cells

Substantial death was observed after first 2 doses of CCCP. At this early stage of depletion some cells rounded up or detached once energy levels fell too low. While next two CCCP doses did not further induce death of the cells. Post depletion, a reduction in cell size was observed, with cells becoming thinner and elongated compared to untreated controls (Figure 3). Loss of mitochondrial biomass leads to stress-induced cytoskeletal remodeling, altered adhesion and spreading. It also leads to disruption of normal organelle arrangement due to autophagic activity causing cytoplasmic crowding and reduction of overall cell volume. After 2 days of recovery in uridine/pyruvate-supplemented media, Rho0 cells maintained viability.

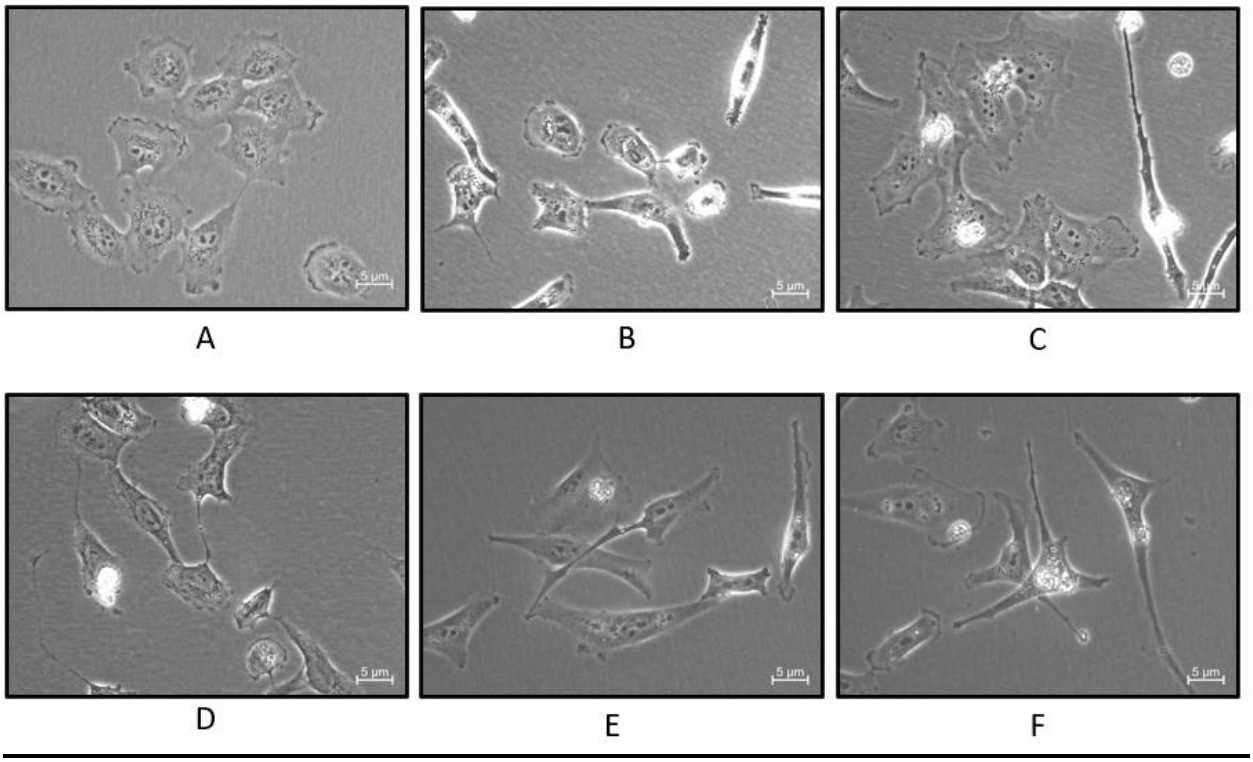

Figure 3. *Morphological changes in MDA-MB-231 Parkin cells during CCCP-induced mitochondrial depletion.* A. Cells before depletion, B. After the 1st dose of CCCP, C. After 2nd dose of CCCP, D. After the 3rd dose of CCCP. E. After the 4th dose of CCCP. F Cells after 2 days in DMEM F-12 supplemented with uridine, and sodium pyruvate.

Treatment with the CCCP successfully induced mitochondrial DNA (mtDNA) depletion in MDA-MB-231 cells, as verified by mtDNA-CN (copy number) analysis.The total cellular DNA was extracted and qPCR was performed using a human mtDNA specific primer ND1 the expression of nuclear DNA encoded HMBS was used as a control. Parental MDA-MB-231 cells exhibited a high mtDNA CN (576.7), while Rho0 cells (passages p1–p3) showed near-complete lack of mtDNA (Table 1).

Table 1. mtDNA Copy Number (MTCN) in MDA-MB-231 Rho0 Cells.

Cell Line	mtDNA-CN (Mean)
MDA-MB-231	576.7
Rho0, p1	0
Rho0, p2	0.67

Rho0, p3	0.015

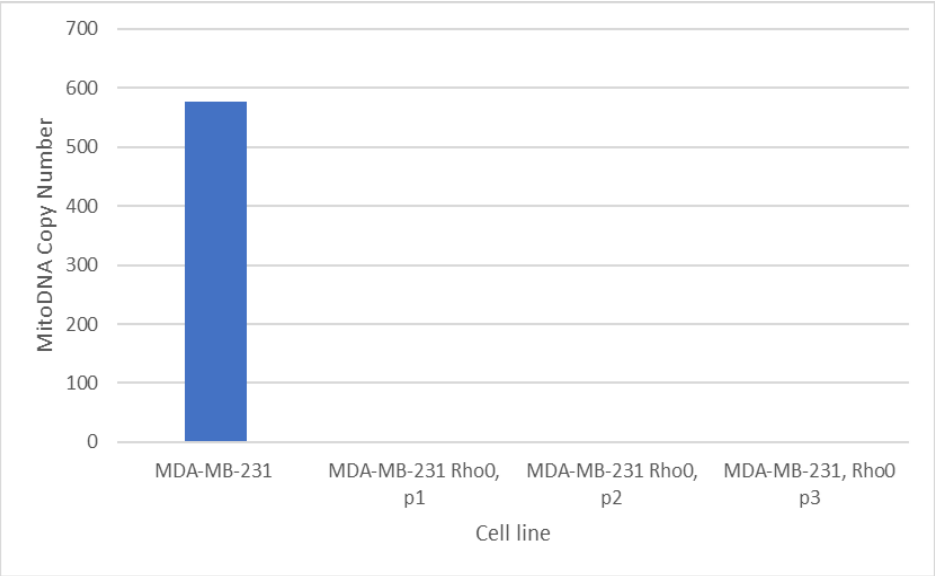

Figure 4. mtDNA Copy Number (MTCN) in MDA-MB-231, and Rho0 Cells.

3.2 MDA-MB 231 Rho0 cells show reduced proliferation rates

Continuous monitoring of cell proliferation using xCELLigence RTCA technology demonstrated significant differences in growth patterns between mitochondrial DNA-depleted (Rho0) and parental MDA-MB-231 cells. The growth kinetics of both cell lines is shown on Figure 4. The Cell Index (CI) curves revealed three distinct phases Initial attachment (t = 0): Rho0: CI = 0.828 ± 0.005, MDA-MB-231: CI = 0.769 ± 0.007 (*p* = 0.15, unpaired *t*-test). Adhesion kinetics (0–2 h): Both lines showed similar CI trajectories (slopes: Rho0 = 0.085 CI/h, MDA-MB-231 = 0.092 CI/h; *p* = 0.32, linear regression). Parental cells exhibited faster proliferation (slope 0.18 CI/hr), compared to Rho0 (slope 0.11CI/hr). By the end of 24 hrs parental cell line reached CI=6.64 vs Rho0=3.94. At plateau phase MDA-MB-231 parental cells maintained higher confluency with CI of 10.04 at 53hr, and Rho0 cells showed 21% lower index (CI=7.96).

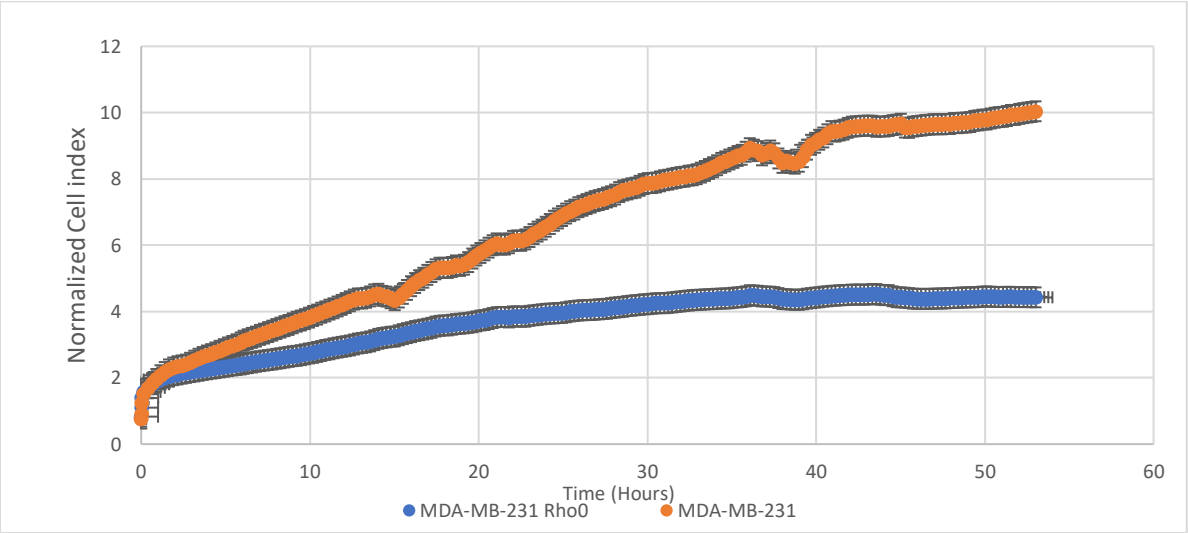

Figure 5. *Proliferation of MDA MB 231 Rho0 cells*

Post-treatment attachment phase (0–2 Hours, Measured Every 15 Minutes)
The xCELLigence system captured cell adhesion dynamics at 15-minute intervals beginning immediately after plating (t = 0 = first measurement post-seeding).

3.3 MTS Assay Reveals Significant Proliferation Defect in Mitochondrial DNA-Depleted Cells

Quantification of cellular metabolic activity via MTS absorbance demonstrated profound differences between parental MDA-MB-231 cells and their Rho0 counterparts at both 24- and 48-hour timepoints (Figure 3).

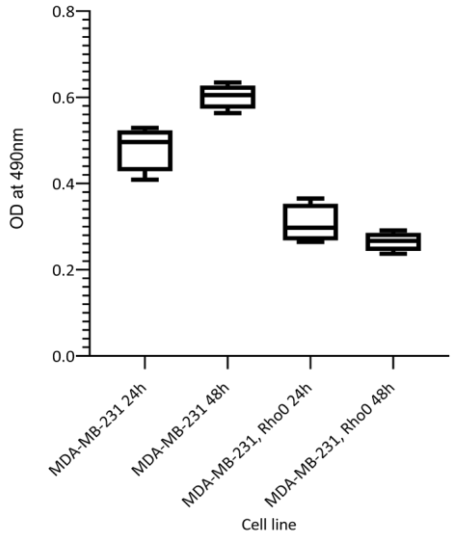

Figure 6. MTS Assay Average absorbance

24-Hour Timepoint: parental cells demonstrated robust metabolic activity (mean ± SD: 0.486 ± 0.049), while Rho0 cells showed 45% reduced activity (0.304 ± 0.046, $p < 0.0001$). The effect size when comparing the proliferation of parental and Rho0 MDA-MB-231s (Cohen's d) was large ($d = 3.89$). At 48-Hour Timepoint the metabolic activity of MDA-MB-231 cells increased by 22% from 24h (0.594 ± 0.045, $p = 0.003$ vs 231 24h). Rho0 cells showed no increase in proliferation(0.263 ± 0.025, $p = 0.12$ vs Rho0 24h), as MDA-MB-231 and Rho0 cell line difference widened to 56% ($p < 0.00001$), the Effect size increased to $d=8.12$ at 48h. Statistical analysis was performed using two-way ANOVA with Šidák's multiple comparisons test.

3.4 Metformin Resistance in Mitochondrial DNA-Depleted Cells

Dose-inhibition analysis revealed significantly reduced sensitivity to metformin in Rho0 cells compared to MDA-MB-231 cells (Figure 6). 24-hour treatment of Metformin on MDA-MB-231 revealed IC_{50} of 19.36 mM (95% CI: 18.12–20.68), for Rho0 IC_{50}=41.05 mM (95% CI: 38.91–43.29). This indicates 2.12-fold higher dose of Metformin was needed for Rho0 cells to achieve similar effect as in MDA-MB-231 cells. At 48h treatment IC_{50} for the parental cell line was 17.6mM (95% CI: 16.35–18.94), and for Rho0 IC_{50} was 23.23mM (96%CI: 21.07-25.61) which was 1.32-fold higher compared to parental cell line:

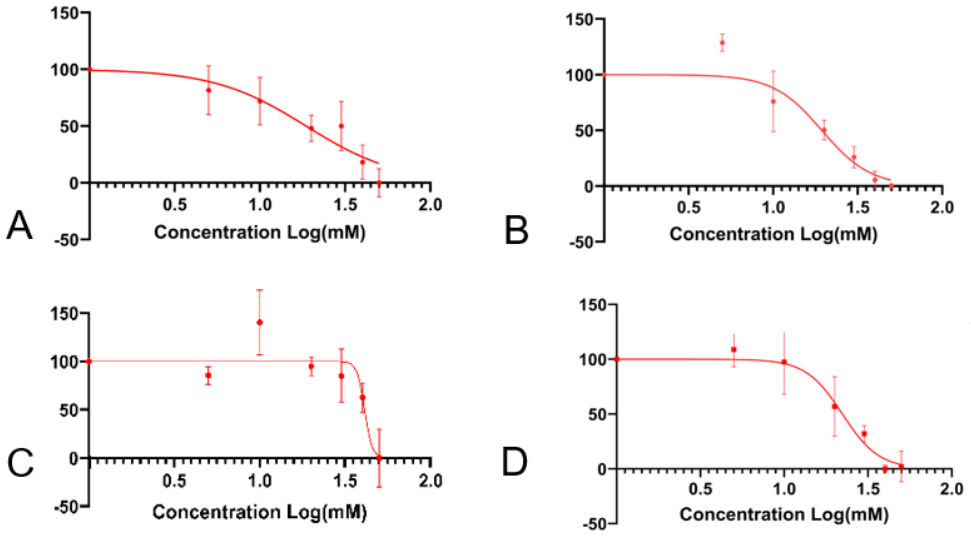

Figure 6. *IC_{50} Dose-inhibition curve.* A. MDA-MB-231 24h Metformin treatment. B. MDA-MB-231 48h Metformin treatment. C MDA-MB-231 Rho0 24h Metformin treatment. D. MDA-MB-231 Rho0 48h Metfromin treatment.

3.5 Confocal imaging of MDA-MB-231, and Rho0 cells with metformin treatment

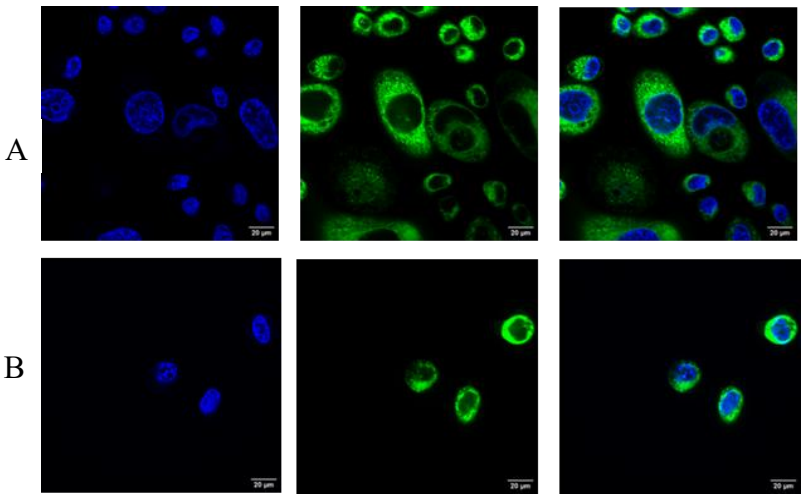

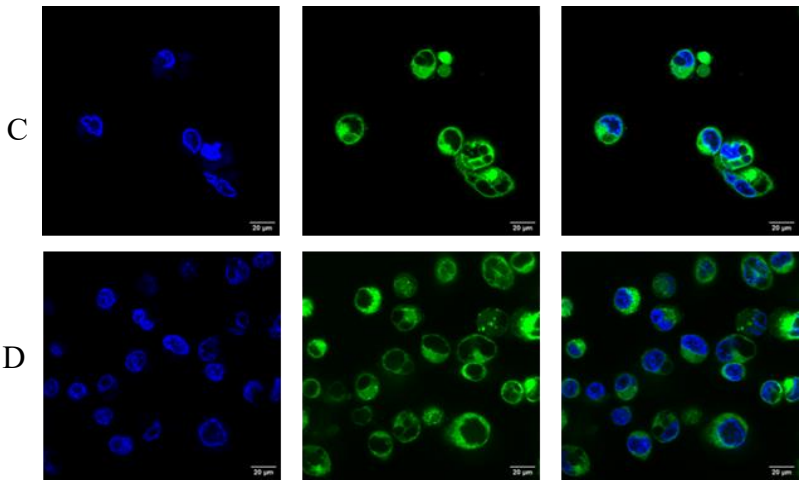

Figure 7. Figure 1. *Morphological comparison of MDA-MB-231, and Rho0 cells with metformin treatment.* A. MDA-MB-231. B. MDA-MB-231+Met. C. MDA-MB-231 Rho0. D. MDA-MB-231 Rho0+Met.

3.6 Xcelligence analysis of Metformin treatment in Rho0 vs parental cells

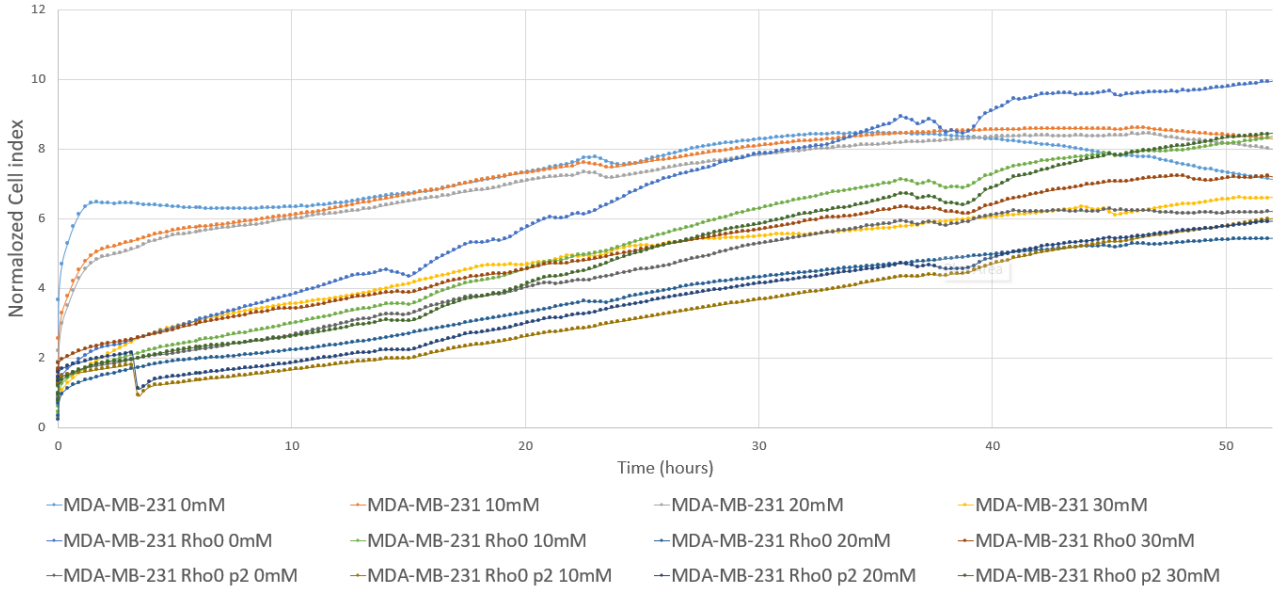

Figure 7 xCELLigence analysis of MDA-MB-231 parental and Rho0 cell lines with Metformin treatment.

MDA-MB-231 parental cells at 0 mM Metformin showed exponential growth (Slope: 0.18 CI/hr) reaching plateau at approximately 30h (CI = 6.45). Metformin-treated cells experienced dose-dependent inhibition at 10-30mM, with 10 mM treatment giving 22% reduction in final CI (*p* < 0.01 vs. 0 mM), and 30 mM exhibited 65% reduction (*p* < 0.0001).

MDAMB-231 Rho0 Cells: basal growth was 38% lower than parental cell line (CI = 4.12 at 30h, *p* < 0.001). Metformin response at 10 mM indicated no significant effect (CI = 3.98, *p* = 0.12), and 30 mM Metformin experienced paradoxical initial CI increase (+113% at 2h) followed by inhibition (40% reduction by 48h).

3.7 Metformin induces ROS production over 24 hours in parental MDA MB 231 but not in Rho0 cells

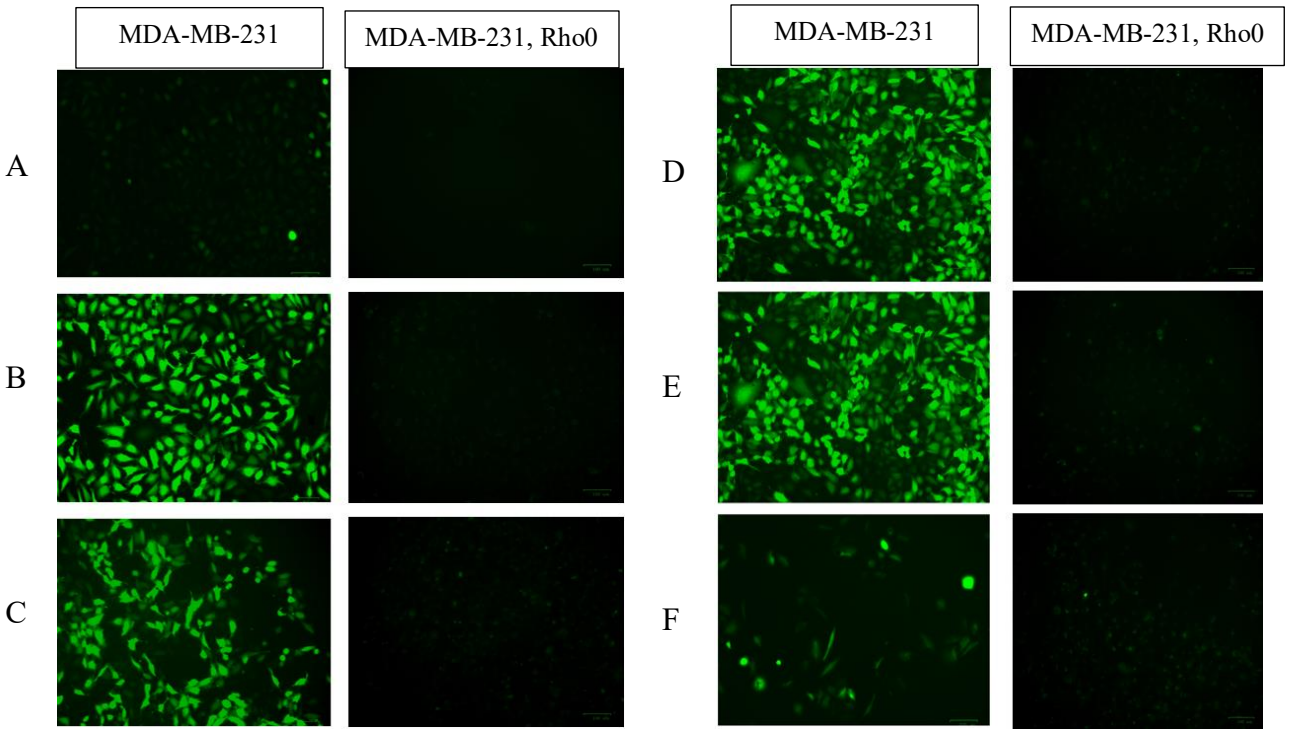

Figure 8. Fluorescence analysis of ROS production of MDA-MB-231, and Rho0 cells with metformin treatment. A. 0mM. B. 5mM. C. 10mM. D. 20mM. E. 40mM. F. 80mM

In the absence of metformin (0 mM),Rho0 cells exhibited significantly higher basal ROS compared to parental cells consistent with their reliance on non-mitochondrial ROS sources due to impaired oxidative phosphorylation (OXPHOS). The ROS response was markedly lower in Rho0 metformin treated cell line, where a slight increase was observed at 5–20 mM, with a peak

at 20 mM. At 40 mM, ROS dropped below basal levels. By 80 mM, ROS partially recovered but consistently remained lower than in metformin-treated parental cells

DISCUSSION

The near-complete mtDNA depletion in Rho0 cells confirms successful enforced mitophagy via CCCP treatment, as previously reported for other cancer cell lines (Correia-Melo et al., 2016). The observed morphological changes (cell thinning, elongation) suggest the link between mtDNA depletion and cellular morphology, with the emphasis on changes in cytoskeleton of the cell. The viability of Rho0 cells in uridine/pyruvate media underscores their dependence on glycolytic metabolism, a hallmark of mitochondrial-depleted cells.

The observed growth retardation in Rho0 cells supports the crucial role of functional mitochondria in cancer cell proliferation: “Disruption of mtDNA resulted in a slower proliferation rate in tissue culture…” (Yu et al., 2007)
Nevertheless, this data establishes that mitochondrial DNA depletion significantly alters BC cell proliferation dynamics, providing a foundation for investigating metabolic adaptation in tumor progression. The 2.3-fold lower metabolic activity in Rho0 cells at 48h aligns with prior reports that MDA-MB-231 cells derive >60% of ATP from oxidative phosphorylation (Jekabsons et al., 2023) despite their glycolytic phenotype (shift to Warburg effect). Failed compensatory glycolysis upregulation suggests critical reliance on mitochondrial ETC (electron transport chain) for NAD+/NADH regeneration, which drives MTS reduction.

4.1 Metformin response. The attenuated metformin response in Rho0 cells supports two non-exclusive mechanisms: action of metformin on mitochondrial complex I, where 2.12-fold higher concentration of metformin were necessary to achieve IC_{50}. And 1.3-fold increased sensitivity at 48h suggests additional, mitochondria-independent effects of metformin on Rho0 cells. Possibly

through: AMPK activation via LKB1, REDD1-mediated mTOR inhibition, and metabolic adaptation.

Qualitative confocal microscopy revealed morphological differences between cell types under 23mM of metformin. MDA-MB-231 Rho0 cells frequently appeared smaller and rounded compared parental cells, suggesting mitochondrial depletion may influence cytoskeletal organization or cell volume regulation. While these observations were not quantified, the consistent phenotypic trend across multiple fields supports a slight biological association.

The dose-dependent ROS induction in parental cells aligns with studies linking metformin to mitochondrial complex I inhibition, elevating superoxide production (Udono & Nishida, 2022). The biphasic pattern suggests: lower doses (5–20 mM): metformin may disrupt electron transport, increasing ROS oxidative effect. 40 mM peak: Potential saturation of antioxidant defenses. Decline at 80 mM, is suggestive with cell death. On the other hand, Rho0 cells' higher basal ROS confirms mitochondrial DNA's role in redox homeostasis. Their reduced response to metformin implies that metformin's primary ROS-generating mechanism requires functional mitochondria (complex I activity).

CONCLUSIONS

This thesis confirms the different antiproliferative effects of metformin on MDA-MB-231, and Rho0 breast cancer cell lines, suggesting that metformin's anti-proliferative effects primarily depend on intact mitochondrial OXPHOS. Throughout this work mitochondrial DNA depletion was successfully optimized, which validated by a complete loss of mtDNA.

In conclusion, this thesis confirms the antiproliferative effect of metformin in MDA-MB-231 breast cancer cell line.

FURTHER SUGGESTIONS

The effect of metformin on other Rho0 breast cancer cell lines should be investigated further. Additional analyses, and pathway investigations would increase our understanding of metformin's underlying effects on Breast cancer cell lines

REAGENTS AND KITS

DMEM/F-12

DMSO, anhydrous (Invitrogen D12345)

PenStrep (15140122, Thermo Fischer Scientific)

L-Glutamine (25030081, Thermo Fischer Scientific)

CCCP (ab141229, Abcam)

Uridine (U3750-25G, Sigma-Aldrich)

Metformin hydrochloride (M1291, CAS No. 1115-70-4, Tokyo Chemical Industry (TCI))

Sodium Pyruvate (P5280, Sigma-Aldrich)

PureLink™ Genomic DNA Mini Kit (K182002, Invitrogen)

SYBR™ Green Universal Master Mix (Applied Biosystems, 4309155).

CellTiter 96® AQ_{ueous} One Solution Cell Proliferation Assay, MTS (Promega, G358A)

E-16 xCelligence plates (300600890, Agilent)

Hoechst (33342, Invitrogen)

xCELLigence RTCA DP - Cell Invasion & Migration (Agilent)

MitoTracker Deep Red FM (M22426, Thermo Fischer Scientific)

REFERENCE LIST

Bailey, C. J. (2017). Metformin: historical overview. *Diabetologia*, *60*(9), 1566–1576. https://doi.org/10.1007/s00125-017-4318-z

Boulton, D. P., & Caino, M. C. (2022). Mitochondrial fission and fusion in tumor progression to metastasis. *Frontiers in Cell and Developmental Biology*, *10*. https://doi.org/10.3389/fcell.2022.849962

Choi, Y. K., & Park, K. (2013). Metabolic roles of AMPK and metformin in cancer cells. *Molecules and Cells*, *36*(4), 279–287. https://doi.org/10.1007/s10059-013-0169-8

Chlebowski, R. T., McTiernan, A., Wactawski-Wende, J., Manson, J. E., Aragaki, A. K., Rohan, T., Ipp, E., Kaklamani, V. G., Vitolins, M., Wallace, R., Gunter, M., Phillips, L. S., Strickler, H., Margolis, K., & Euhus, D. M. (2012). Diabetes, metformin, and BC in postmenopausal women. *Journal of Clinical Oncology*, *30*(23), 2844–2852. https://doi.org/10.1200/jco.2011.39.7505

Correia-Melo, C., Ichim, G., Tait, S. W. G., & Passos, J. F. (2016). Depletion of mitochondria in mammalian cells through enforced mitophagy. *Nature Protocols*, *12*(1), 183–194. https://doi.org/10.1038/nprot.2016.159

Dai, X., Cheng, H., Bai, Z., & Li, J. (2017). BC Cell Line Classification and Its Relevance with Breast Tumor Subtyping. *Journal of Cancer*, *8*(16), 3131–3141. https://doi.org/10.7150/jca.18457

Dunenova. A, D., ZhA, K., DR, K., OV, S., AZh, Z., EA, M., AA, D., RI, F., & NE, G. (2023). BC EPIDEMIOLOGY IN KAZAKHSTAN FOR THE PERIOD 2012-2021. *Наука И Здравоохранение*, *2(25)*, 128–137. https://doi.org/10.34689/sh.2023.25.2.018

Gilkerson, R. W., Margineantu, D. H., Capaldi, R. A., & Selker, J. M. (2000). Mitochondrial DNA depletion causes morphological changes in the mitochondrial reticulum of cultured human cells. *FEBS Letters*, *474*(1), 1–4. https://doi.org/10.1016/s0014-5793(00)01527-1

Jekabsons, M. B., Merrell, M., Skubiz, A. G., Thornton, N., Milasta, S., Green, D., Chen, T., Wang, Y., Avula, B., Khan, I. A., & Zhou, Y. (2023). BC cells that preferentially metastasize to lung or bone are more glycolytic, synthesize serine at greater rates, and consume less ATP and NADPH than parent MDA-MB-231 cells. *Cancer & Metabolism*, *11*(1). https://doi.org/10.1186/s40170-023-00303-5

Hanahan, D. (2022). Hallmarks of Cancer: New Dimensions. *American Association of Cancer Research*, *12*(1), 31–46. https://doi.org/10.1158/2159-8290.CD-21-1059

Hera Biolabs. (2023, April 26). *The MCF-7 BC Model: A Definitive guide*. Hera BioLabs. https://www.herabiolabs.com/the-mcf-7-breast-cancer-model-a-definitive-guide/

Khozhukhar, N., Spadafora, D., Rodriguez, Y. a. R., Fayzulin, R., & Alexeyev, M. (2023). Generation of Mammalian Cells Devoid of Mitochondrial DNA (ρ0 cells). *Current Protocols*, *3*(2). https://doi.org/10.1002/cpz1.679

Kim, H. J., Kwon, H., Lee, J. W., Kim, H. J., Lee, S. B., Park, H. S., Sohn, G., Lee, Y., Koh, B. S., Yu, J. H., Son, B. H., & Ahn, S. H. (2015). Metformin increases survival in hormone receptor-positive, HER2-positive BC patients with diabetes. *BC Research*, *17*(1). https://doi.org/10.1186/s13058-015-0574-3

King, M. P., & Attardi, G. (1989). Human Cells Lacking mtDNA: Repopulation with Exogenous Mitochondria by Complementation. *Science*, *246*(4929), 500–503. https://doi.org/10.1126/science.2814477

Lee, Y. G., Park, D. H., & Chae, Y. C. (2022). Role of mitochondrial stress response in cancer progression. *Cells*, *11*(5), 771. https://doi.org/10.3390/cells11050771

Lega, I. C., Austin, P. C., Gruneir, A., Goodwin, P. J., Rochon, P. A., & Lipscombe, L. L. (2013). Association between metformin therapy and mortality after BC. *Diabetes Care*, *36*(10), 3018–3026. https://doi.org/10.2337/dc12-2535

Livak, K. J., & Schmittgen, T. D. (2001). Analysis of relative gene expression data using Real-Time Quantitative PCR and the 2−ΔΔCT method. *Methods*, *25*(4), 402–408. https://doi.org/10.1006/meth.2001.1262

Łukasiewicz, S., Czeczelewski, M., Forma, A., Baj, J., Sitarz, R., & Stanisławek, A. (2021). BC—Epidemiology, Risk factors, Classification, Prognostic Markers, and Current Treatment Strategies—An Updated Review. *Cancers*, *13*(17), 4287. https://doi.org/10.3390/cancers13174287

Ma, Y., Wang, L., & Jia, R. (2020, May 1). *The role of mitochondrial dynamics in human cancers*. https://pmc.ncbi.nlm.nih.gov/articles/PMC7269774/#:~:text=For%20example%2C%20mitochondrial%20dynamics%20regulates,their%20nonmetastatic%20counterparts%20%5B61%5D.

Midlenko, A., Mussina, K., Zhakhina, G., Sakko, Y., Rashidova, G., Saktashev, B., Adilbay, D., Shatkovskaya, O., & Gaipov, A. (2023). Prevalence, incidence, and mortality rates of BC in Kazakhstan: data from the Unified National Electronic Health System, 2014–2019. *Frontiers in Public Health*, *11*. https://doi.org/10.3389/fpubh.2023.1132742

Moldasheva, A., Zhakupova, A., & Aljofan, M. (2024). Antiproliferative mechanisms of metformin in breast cancer: A Systematic review of the literature. *International Journal of Molecular Sciences*, *26*(1), 247. https://doi.org/10.3390/ijms26010247

Qu, Y., Han, B., Yu, Y., Yao, W., Bose, S., Karlan, B. Y., Giuliano, A. E., & Cui, X. (2015). Evaluation of MCF10A as a reliable model for normal human mammary epithelial cells. *PLoS ONE*, *10*(7), e0131285. https://doi.org/10.1371/journal.pone.0131285

Sung, H., Ferlay, J., Siegel, R. L., Laversanne, M., Soerjomataram, I., Jemal, A., & Bray, F. (2021). Global Cancer Statistics 2020: GLOBOCAN estimates of incidence and mortality

worldwide for 36 cancers in 185 countries. *CA a Cancer Journal for Clinicians*, *71*(3), 209–249. https://doi.org/10.3322/caac.21660

Udono, H., & Nishida, M. (2022). Metformin-ROS-Nrf2 connection in the host defense mechanism against oxidative stress, apoptosis, cancers, and ageing. *Biochimica Et Biophysica Acta (BBA) - General Subjects*, *1866*(8), 130171. https://doi.org/10.1016/j.bbagen.2022.130171

Wallace, D. C. (1999). Mitochondrial diseases in man and mouse. *Science*, *283*(5407), 1482–1488. https://doi.org/10.1126/science.283.5407.1482

Wallace, D. C. (2012). Mitochondria and cancer. *Nature Reviews. Cancer*, *12*(10), 685–698. https://doi.org/10.1038/nrc3365

Welsh, J. (2013). Animal models for studying prevention and treatment of BC. In *Elsevier eBooks* (pp. 997–1018). https://doi.org/10.1016/b978-0-12-415894-8.00040-3

Xing, J., Qi, L., Liu, X., Shi, G., Sun, X., & Yang, Y. (2022). Roles of mitochondrial fusion and fission in BC progression: a systematic review. *World Journal of Surgical Oncology*, *20*(1). https://doi.org/10.1186/s12957-022-02799-5

Yu, M., Shi, Y., Wei, X., Yang, Y., Zhou, Y., Hao, X., Zhang, N., & Niu, R. (2007). Depletion of mitochondrial DNA by ethidium bromide treatment inhibits the proliferation and tumorigenesis of T47D human BC cells. *Toxicology Letters*, *170*(1), 83–93. https://doi.org/10.1016/j.toxlet.2007.02.013

Yu, S., Kim, T., Yoo, K. H., & Kang, K. (2017). The T47D cell line is an ideal experimental model to elucidate the progesterone-specific effects of a luminal A subtype of BC. *Biochemical and Biophysical Research Communications*, *486*(3), 752–758. https://doi.org/10.1016/j.bbrc.2017.03.114

Zhuang, Y., & Miskimins, W. K. (2011). Metformin induces both Caspase-Dependent and Poly(ADP-ribose) Polymerase-Dependent cell death in BC cells. *Molecular Cancer Research*, *9*(5), 603–615. https://doi.org/10.1158/1541-7786.mcr-10-0343